

## TECHNICAL REPORT

# Optimized 14 + 1 receive coil array and position system for 3D high-resolution MRI of dental and maxillomandibular structures

<sup>1</sup>Jan Sedlacik, <sup>1</sup>Daniel Kutzner, <sup>1</sup>Arun Khokale, <sup>1</sup>Dirk Schulze, <sup>1</sup>Jens Fiehler, <sup>2</sup>Turgay Celik, <sup>2</sup>Daniel Gareis, <sup>3</sup>Ralf Smeets, <sup>3</sup>Reinhard E Friedrich, <sup>3</sup>Max Heiland and <sup>3</sup>Alexandre T Assaf

<sup>1</sup>Department of Diagnostics and Interventional Neuroradiology, University Medical Center Hamburg Eppendorf, University of Hamburg, Hamburg, Germany; <sup>2</sup>NORAS MRI products GmbH, Höchberg, Germany; <sup>3</sup>Department of Oral and Maxillofacial Surgery, University Medical Center Hamburg Eppendorf, University of Hamburg, Hamburg, Germany

**Objectives:** The purpose of this study was to design, build and test a multielement receive coil array and position system, which is optimized for three-dimensional (3D) high-resolution dental and maxillomandibular MRI with high patient comfort.

**Methods:** A 14 + 1 coil array and positioning system, allowing easy handling by the technologists, reproducible positioning of the patients and high patient comfort, was tested with three healthy volunteers using a 3.0-T MRI machine (Siemens Skyra; Siemens Medical Solutions, Erlangen, Germany). High-resolution 3D  $T_1$  weighted, water excitation  $T_1$  weighted and fat-saturated  $T_2$  weighted imaging sequences were scanned, and 3D image data were reformatted in different orientations and curvatures to aid diagnosis.

**Results:** The high number of receiving coils and the comfortable positioning of the coil array close to the patient's face provided a high signal-to-noise ratio and allowed high quality, high resolution, 3D image data to be acquired within reasonable scan times owing to the possibility of parallel image acquisition acceleration. Reformatting the isotropic 3D image data in different views is helpful for diagnosis, e.g. panoramic reconstruction. The visibility of soft tissues such as the mandibular canal, nutritive canals and periodontal ligaments was exquisite.

**Conclusions:** The optimized MRI receive coil array and positioning system for dental and oral-maxillofacial imaging provides a valuable tool for detecting and diagnosing pathologies in dental and oral-maxillofacial structures while avoiding radiation dose. The high patient comfort, as achieved by our design, is very crucial, since image artefacts due to movement or failing to complete the examination jeopardize the diagnostic value of MRI examinations.

*Dentomaxillofacial Radiology* (2016) **45**, 20150177. doi: [10.1259/dmfr.20150177](https://doi.org/10.1259/dmfr.20150177)

**Cite this article as:** Sedlacik J, Kutzner D, Khokale A, Schulze D, Fiehler J, Celik T, et al. Optimized 14 + 1 receive coil array and position system for 3D high-resolution MRI of dental and maxillomandibular structures. *Dentomaxillofac Radiol* 2016; **45**: 20150177.

**Keywords:** dental pulp; periodontal ligament; apical foramen; salivary glands

## Introduction

MRI depicts soft tissues with great detail and contrast. Dental or maxillomandibular pathologies can cause soft-tissue alteration before distinct destruction of osseous structures. Therefore, MRI may allow these pathologies to be assessed at a very early stage. However,

MRI is not common in dentistry or oral-maxillofacial surgery. Earlier studies on dental MRI investigated its diagnostic value<sup>1,2</sup> or focused only on high-resolution imaging of the teeth.<sup>3</sup> So far, no study focused on making dental MRI feasible for clinical routine by optimizing the MRI coils or developing comfortable positioning system and dental MRI sequences. State-of-the-art routine MRI systems with 3.0-T magnetic field strength and the capability of accelerated image

Correspondence to: Jan Sedlacik. E-mail: [j.sedlacik@uke.uni-hamburg.de](mailto:j.sedlacik@uke.uni-hamburg.de)

This study was supported by German Federal Ministry for Economic Affairs and Energy, Central Innovation Program for SMEs (ZIM), KF3259801CS3. Received 21 May 2015; revised 5 August 2015; accepted 9 September 2015

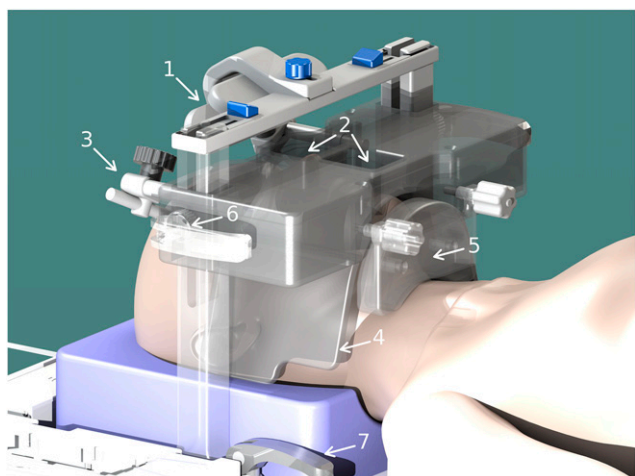


**Figure 1** Rendered computer-aided drafting model of the mandibular coil array and positioning system with mirror (1), wide openings for mouth and nose (2), head fixation (3), flexible coil array wings (4), adjustable rigid lower jaw coil element (5) and fasteners for positioning (6,7).

acquisition<sup>4</sup> allow high spatial resolution with sufficient signal-to-noise ratio and reasonable scan times which are essential for dental MRI. We recently explored the capability of current clinical MRI machines for dental imaging.<sup>2</sup> We found excellent visualization of dental or maxillo-mandibular soft-tissue structures. However, dental MRI with satisfactory image quality and high patient comfort is challenging without specifically optimized equipment for dental MRI.

Therefore, the purpose of our work was to design, build and test a multielement receive coil array and

position system optimized for three-dimensional (3D) high-resolution dental and maxillo-mandibular MRI with high patient comfort.

## Methods and materials

The 14 + 1 coil array and positioning system (Figure 1) consists of a curved  $12 \times 38\text{-cm}^2$ , 14-element phased-array coil mounted between two pillars. Fasteners on the bottom of the pillars allow positioning in head-foot direction and fasteners between the pillars and the rigid body of the coil allow anteroposterior positioning. The centre of the phased-array coil provides wide openings for nose and mouth. The central junction between the two openings is positioned directly above the patient's upper lip. The outer wings of the phased-array coil are highly flexible and can be perfectly adapted to the individual anatomy. One butterfly coil element attached to the inferior side of the rigid body of the coil array provides additional coverage and support to the lower jaw. The butterfly element can be freely adjusted to the individual anatomy. Optional mirror and head fixation can also be attached to increase patient comfort and to further minimize head motion. In particular the mirror by allowing the patient to look outside of the magnet bore, is a very efficient way to comfort and calm patients with claustrophobia. The head was placed on a standard foam headrest, but also vacuum cushions can be used. The high number of receive elements allows for accelerated data acquisition owing to parallel imaging and subsequent  $k$ -space undersampling. This makes high-resolution 3D imaging with reasonable scan times

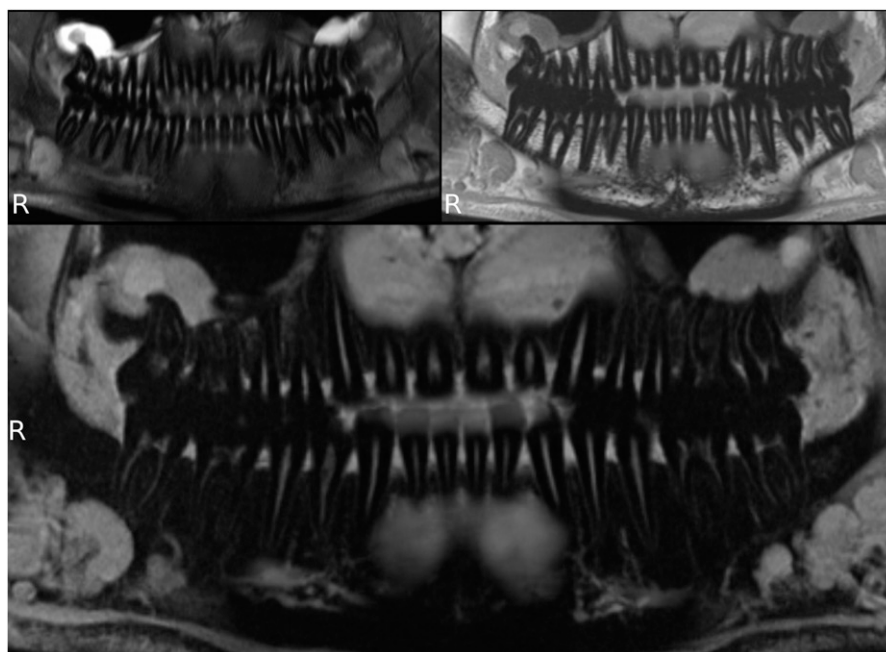


**Figure 2** Panoramic reconstructions of three-dimensional image data; fat saturation  $T_2$  weighted (top left),  $T_1$  weighted (top right) and water excitation  $T_1$  weighted (bottom).

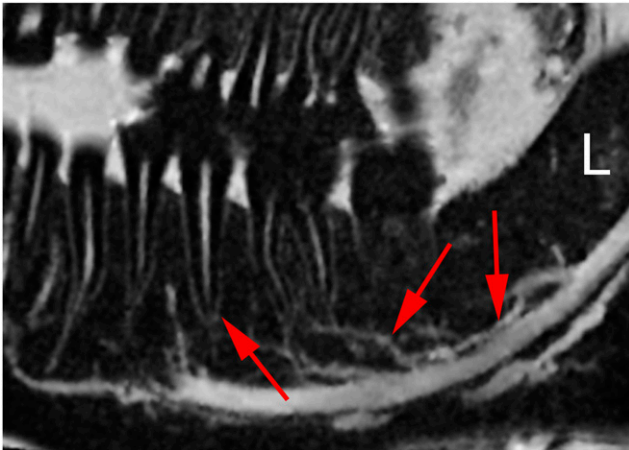


**Figure 3** Detail of lower jaw with mandibular canal (right arrow), nutritive canals (middle arrow), periodontal ligament and apical foramen (left arrow) (water excitation  $T_1$  weighted).

feasible for routine MRI and tolerable by the patient. MRI imaging parameters were:

**Fat saturation  $T_2$  weighted (fsT2w):**  $T_2$  weighted turbo spin echo with variable flip angles, spectral fat saturation and restoring of longitudinal magnetization with echo time/repetition time = 172/1500 ms, turbo factor = 100, matrix =  $384 \times 384 \times 208$ , voxel size =  $0.5 \times 0.5 \times 0.5 \text{ mm}^3$ , readout bandwidth = 355 Hz per pixel, acceleration factor = 2, reference lines = 24, partial Fourier of 6/8 in phase- and slice-encoding directions, 50% slice resolution and acquisition duration = 5 : 15 min.

**$T_1$  weighted (T1w):**  $T_1$  weighted spoiled gradient-echo imaging with echo time/repetition time = 2.46/5.8 ms, matrix =  $384 \times 384 \times 208$ , voxel size =  $0.5 \times 0.5 \times 0.5 \text{ mm}^3$ , readout bandwidth = 345 Hz per pixel, acceleration factor = 2, reference lines = 24, partial Fourier of 6/8 in phase- and slice-encoding directions and acquisition duration = 3 : 06 min.

**Water excitation  $T_1$  weighted (weT1w):**  $T_1$  weighted spoiled gradient-echo imaging with water excitation

for fat suppression with echo time/repetition time = 5.37/10.6 ms, matrix =  $480 \times 480 \times 208$ , voxel size =  $0.375 \times 0.375 \times 0.375 \text{ mm}^3$ , readout bandwidth = 250 Hz per pixel, acceleration factor = 2, reference lines = 24, partial Fourier of 6/8 in phase- and slice-encoding directions and acquisition duration = 6 : 57 min.

All sequences were scanned in axial orientation, with the 3D image slab centred at the approximate plane of centric occlusion. Holding the lower jaw closed was supported by the lower jaw coil element. The whole MRI examination took about 25 min including patient and coil positioning, localization and placing of the 3D image slabs as well as automatic adjustment scans of the MRI system. For comparison of image quality with the standard head and neck coil, MRI sequences were acquired with the same imaging parameters and reviewed in comparison with the images of the newly developed coil by an experienced dental radiologist (DS). A scoring system with 1 (excellent), 2 (good), 3 (moderate), 4 (poor) and 5 (not visible) was applied according to our previous work.<sup>2</sup> The scores for the different coils and MRI sequences were statistically compared by two-factor ANOVA with the level of significance of  $p = 0.05$ .

3D image data were post-processed, *e.g.* by curved and oblique planar reconstructions, using the OnDemand3D software (Cybermed Inc., Seoul, Korea).

Three healthy volunteers without pathological dental or maxillomandibular findings were scanned using the 14 + 1 coil array and positioning system with a 3.0-T MRI (Siemens Skyra; Siemens Medical Solutions, Erlangen, Germany). No volunteer had metal implants which could potentially deteriorate image quality. One volunteer had amalgam fillings on all molar teeth, and one volunteer had one root canal treatment of tooth 34. All subjects gave written informed consent consistent with the Declaration of Helsinki in its currently applicable form, which was approved by the local ethics committee.

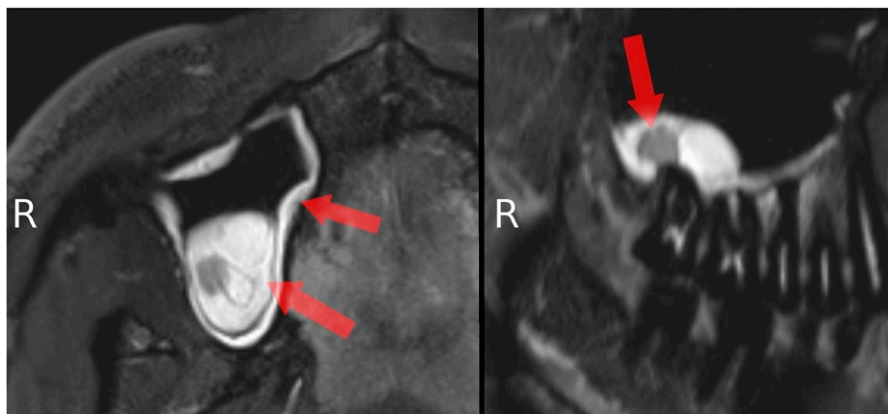


**Figure 4** Detail of upper jaw and adjacent maxillary sinus: mucosal thickening (left arrows) and cystic lesion (right arrow) (fat saturation  $T_2$  weighted).



**Figure 5** Detail of the lower first molar (start of arrow) and three-dimensional segmentation (end of arrow) of its pulp chamber (fat saturation  $T_2$  weighted).

## Results

All volunteers reported high comfort at all times of the examination. The head and coil positioning did not cause any discomfort, *e.g.* pressure to the cheekbones or extension of the neck. Patient and coil positioning was easy and reproducible between examinations and subjects. 3D isotropic image data of all three sequences were of high quality, and post-processing with adequate software tools allows reconstruction of different views which are helpful for diagnosis, *e.g.* panoramic reconstruction (Figure 2). The visibility of the mandibular canal, nutritive canals and periodontal ligaments was exquisite. Especially for the high-resolution  $wT1w$  data, the apical foramen could be assessed (Figure 3). Soft tissues regarding potential pathological conditions and their relationship to surrounding structures could clearly be depicted, as demonstrated in one volunteer with the incidental finding of mucosal thickening and cystic lesion (Figure 4). The  $fsT2w$  data showed great visibility of the pulp chamber,

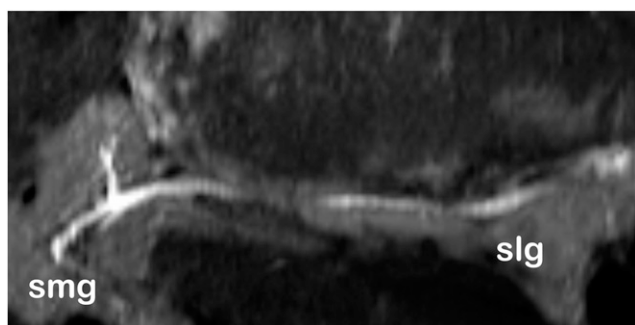


**Figure 6** Submandibular (smg) and sublingual (slg) salivary glands and ducts at low salivation rate (fat saturation  $T_2$  weighted).

which may allow better diagnosis of inflammation and the vitality of the pulp (Figure 5). Furthermore, salivary glands and ducts were also depicted in great detail and with very good delineation against surrounding structures (Figures 6 and 7).

The comparison of image quality and visibility of dental and maxillo-mandibular structures showed better image quality and visibility of the new coil (Figure 8). Scoring of the dental and maxillo-mandibular structures gave consistently and statistically significant ( $p = 0.019$ ) lower (better) scores for the new coil. The scoring was not found to be significantly different ( $p = 0.57$ ) between the different MRI sequences, as well as the interaction between the two factors (coils and sequences) ( $p = 0.96$ ) (Table 1).

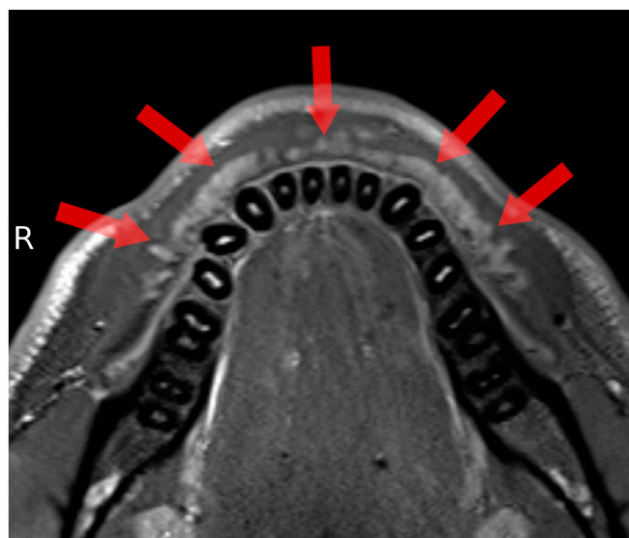


**Figure 7** Small salivary glands (arrows) in the buccal mucosa (fat saturation  $T_2$  weighted).

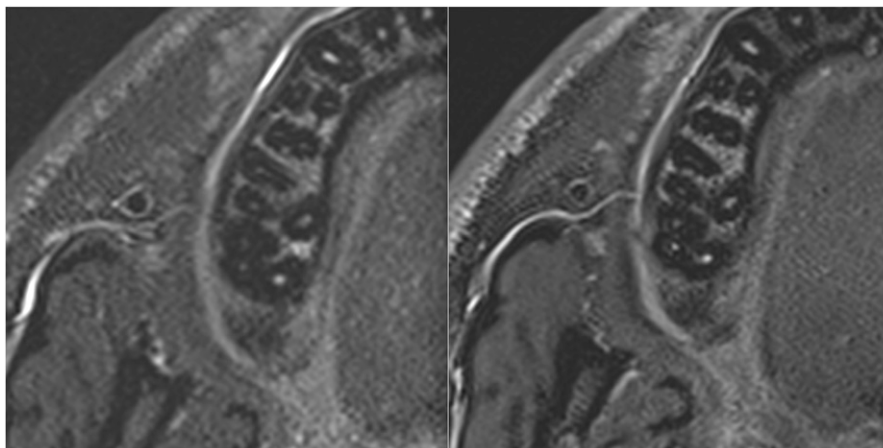


**Figure 8** Exemplary comparison of image quality between standard (left) and new (right) coil. In particular, more details are visible in the images of the new coil.

### Discussion

The goal of our work was to design, build and test a dental and maxillomandibular MRI coil array and position system with high patient comfort that was capable of 3D high-resolution imaging with high image quality at reasonable scan times. High patient comfort and image quality was achieved by designing the coil array and its flexible elements to be positioned as close as possible to the individual anatomy without causing discomfort, *e.g.* pressure to the cheekbones or extension of the neck. Standard MRI coils do not have this ability. For example, the patient’s head needs to be positioned with an extended neck to bring the jaw close to the elements of a standard head and neck coil.<sup>2</sup> Standard flexible coil arrays have no suitable openings for mouth, nose and eyes and may exert intolerable pressure to the patient’s face because of the missing coil supporting structure.

The butterfly element of our coil, covering and supporting the lower jaw, further improves patient

comfort. It prevents the patient from unconsciously opening the mouth or constantly exerting the masseter in order to keep the mouth closed during the examination. This makes additional uncomfortable jaw fixations or restrains, such as a head–chin bandage<sup>2</sup> or a mouth piece, obsolete. The butterfly element can also be retracted to allow for open mouth temporomandibular joint imaging.

Owing to the high spatial resolution and signal provided by the optimized coil design, salivary glands and ducts can be sufficiently depicted at their native low salivation rate. There is no need to enhance salivation, *e.g.* by applying an oral sialogogue such as lemon juice,<sup>5</sup> which may cause patient discomfort and even image artefacts due to uncontrolled swallowing movements.

The optimized coil array and position system opens the possibility for high quality and even quantitative<sup>6</sup> dental and oral–maxillofacial imaging studies as well as for routine diagnostics, where soft-tissue contrast and/or avoidance of radiation dose is of high importance.

**Table 1** Rating of visibility of different dental and maxillomandibular structures in comparison between the newly developed coil and the previously used standard head and neck coil<sup>2</sup>

<i>Anatomical and dental structures</i>	<i>New coil</i>			<i>Standard head/neck coil</i>		
	<i>fsT2w</i>	<i>T1w</i>	<i>weT1w</i>	<i>fsT2w</i>	<i>T1w</i>	<i>weT1w</i>
<b>Anatomical structures</b>						
Cortical and trabecular bone of the mandible and maxilla	2	1	3	3	3	4
Mandibular nerve canal with its nerve structures and mental foramen	3	2	2	4	2	2
Lingual nerve	3	2	4	5	3	4
Salivary glands and their excretory duct	2	3	3	3	4	4
Surrounding soft tissues regarding any pathologies (maximum sinuses)	1	2	2	2	2	3
<b>Dental structures</b>						
Enamel–dentine junction	5	5	5	5	5	5
Cementum–dentine junction of the teeth–pulp chamber	2	3	3	3	4	3
Apical foramen	5	2	3	5	4	4
Periodontal space	5	4	3	5	5	5

fsT2w, fat saturated  $T_2$  weighted; T1w,  $T_1$  weighted; weT1w, water excitation  $T_1$  weighted. Two-factor ANOVA showed statistically significant ( $p = 0.019$ ) better (lower) scores (80 vs 101) for the new coil.

Since no volunteer had appreciable metal implants, no image deterioration was caused because of that. Metallic implants, such as fixtures or retainers, cause severe image artefacts which are not reduced by just using the newly developed coil. However, the increased signal sensitivity of the coil may be helpful for implementing future imaging sequences which are less sensitive to metal artefacts. Such sequences need very high excitation and receiving bandwidths, which lower their signal sensitivity, but may be compensated by the higher signal sensitivity of the new coil.

## Conclusions

The optimized MRI receive coil array and positioning system for dental and oral-maxillofacial imaging allows for high-quality 3D high-spatial resolution imaging with reasonable scan times using a 3.0-T MRI machine. This

provides a valuable tool for detecting and diagnosing pathologies in dental and oral-maxillofacial structures while avoiding radiation dose. The coil array and positioning system is easy to handle and provides high patient comfort. Patient comfort is of high importance, since image artefacts due to movement or failing to complete the examination jeopardize the diagnostic value of the MRI examinations.

## Acknowledgments

The authors thank Olga Tymofiyeva, Department of Radiology and Biomedical Imaging, University of California San Francisco, San Francisco, CA, USA, for helpful discussion and comments on the design of the coil array and the positioning system, and Siemens Healthcare for providing an additional coil adapter interface for the third party coils.

## References

1. Kress B, Gottschalk A, Schmitter M, Sartor K. Benign diseases of the mandible in MRI. [In German.] *Rofo* 2004; **176**: 491–9.
2. Assaf AT, Zrnc TA, Remus CC, Schönfeld M, Habermann CR, Riecke B, et al. Evaluation of four different optimized magnetic-resonance-imaging sequences for visualization of dental and maxillo-mandibular structures at 3 T. *J Craniomaxillofac Surg* 2014; **42**: 1356–63. doi: [10.1016/j.jcms.2014.03.026](https://doi.org/10.1016/j.jcms.2014.03.026)
3. Tymofiyeva O, Boldt J, Rottner K, Schmid F, Richter EJ, Jakob PM. High-resolution 3D magnetic resonance imaging and quantification of carious lesions and dental pulp *in vivo*. *MAGMA* 2009; **22**: 365–74. doi: [10.1007/s10334-009-0188-9](https://doi.org/10.1007/s10334-009-0188-9)
4. Deshmane A, Gulani V, Griswold MA, Seiberlich N. Parallel MR imaging. *J Magn Reson Imaging* 2012; **36**: 55–72. doi: [10.1002/jmri.23639](https://doi.org/10.1002/jmri.23639)
5. Habermann CR, Graessner J, Cramer MC, Aldefeld D, Reitmeier F, Weiss F, et al. MR-sialography: optimisation and evaluation of an ultra-fast sequence in parallel acquisition technique and different functional conditions of salivary glands. [In German.] *Rofo* 2005; **177**: 543–9. doi: [10.1055/s-2005-858040](https://doi.org/10.1055/s-2005-858040)
6. Kress B, Buhl Y, Anders L, Stippich C, Palm F, Bähren W, et al. Quantitative analysis of MRI signal intensity as a tool for evaluating tooth pulp vitality. *Dentomaxillofac Radiol* 2004; **33**: 241–4. doi: [10.1259/dmfr/33063878](https://doi.org/10.1259/dmfr/33063878)